NASA TECHNICAL NOTE

NASA TN D-4536

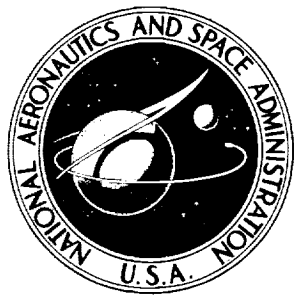

NASA TN D-4536

AN INVESTIGATION OF THE HELICOPTER HEIGHT-VELOCITY DIAGRAM SHOWING EFFECTS OF DENSITY ALTITUDE AND GROSS WEIGHT

by Robert J. Pegg

Langley Research Center

Langley Station, Hampton, Va.

NATIONAL AERONAUTICS AND SPACE ADMINISTRATION • WASHINGTON, D. C. • MAY 1968

NASA TN D-4536

AN INVESTIGATION OF THE HELICOPTER HEIGHT-VELOCITY DIAGRAM SHOWING EFFECTS OF DENSITY ALTITUDE AND GROSS WEIGHT

By Robert J. Pegg

Langley Research Center
Langley Station, Hampton, Va.

NATIONAL AERONAUTICS AND SPACE ADMINISTRATION

For sale by the Clearinghouse for Federal Scientific and Technical Information
Springfield, Virginia 22151 – CFSTI price $3.00

AN INVESTIGATION OF THE HELICOPTER HEIGHT-VELOCITY DIAGRAM SHOWING EFFECTS OF DENSITY ALTITUDE AND GROSS WEIGHT

By Robert J. Pegg
Langley Research Center

SUMMARY

Within the limitations of the available data, this report is intended to provide a method by which experimentally determined helicopter height-velocity diagrams may be modified to show the effects of density altitude and gross weight.

Variations in the established height-velocity diagram can be predicted for changes in density altitude and gross weight by using a generalized nondimensional curve. This generalized curve is based on semiempirical functions derived from flight-test data. During the flight testing of new helicopter designs, this semiempirical method can be used advantageously to predict changes in autorotation characteristics. This method can also predict the approximate shape of the height-velocity diagram while preliminary designs of a helicopter are being made.

To illustrate the use of the semiempirical procedure, a detailed numerical example is given. The step-by-step calculations show the use of the curves and equations.

INTRODUCTION

The capability of a helicopter to perform a safe autorotative landing after a power failure is limited by the structural and aerodynamic design of the particular helicopter for certain combinations of geometric height and airspeed. Power failure within the dangerous region defined by these combinations of geometric height and airspeed results in high risk of severe damage to the aircraft and injury to the occupants. These limiting combinations of airspeed and height are best expressed as the height-velocity diagram shown in figure 1.

For many years there has been a need for a reliable method by which the height-velocity diagram could be treated analytically for any helicopter. Investigations such as those of references 1 to 3 were made in an attempt to solve this problem, but only recently has there been sufficiently accurate flight data available to aid in the modification of the existing work. Systematic experimental measurements of the height-velocity

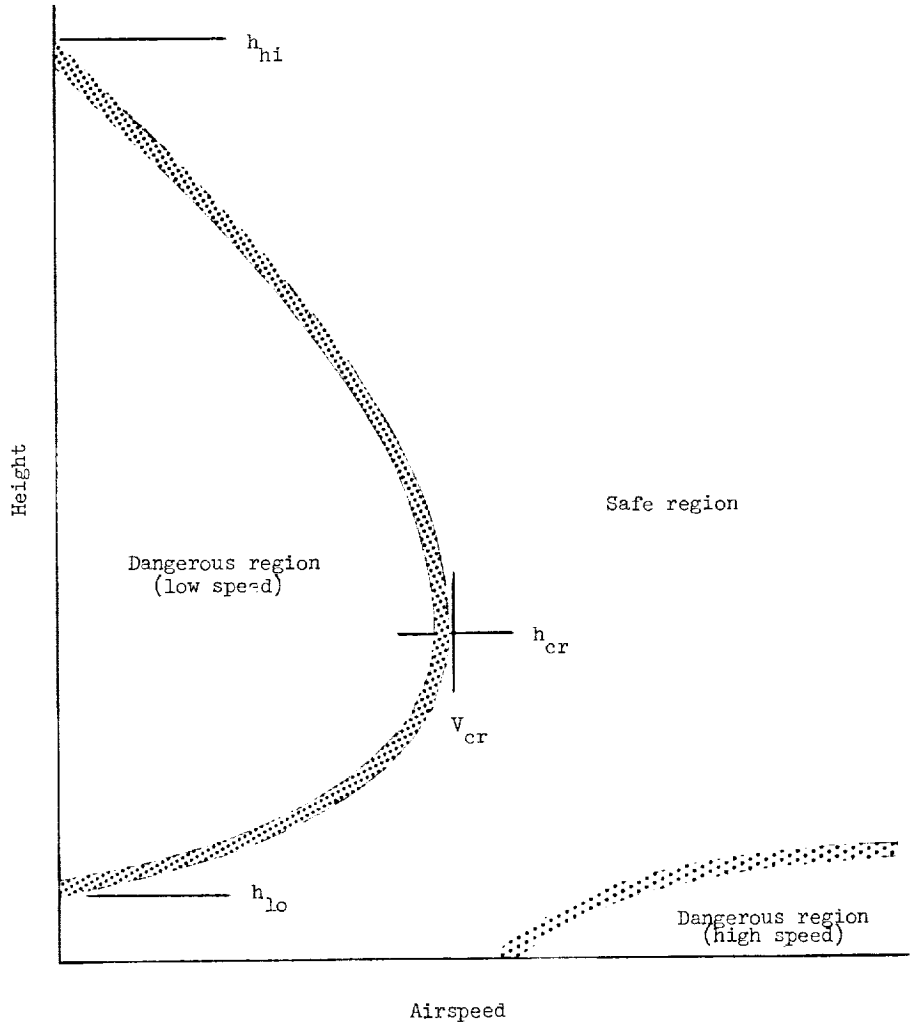

Figure 1.- Typical height-velocity diagram.

diagram were carried out by the Federal Aviation Agency (FAA). The results of these programs are reported in references 4 to 6 and are summarized in reference 7.

The purpose of the current report is to present a semiempirical procedure which shows the effects of density altitude (the altitude corresponding to a given density in the standard atmosphere) and gross weight on the height-velocity diagrams for generally similar single-rotor helicopters. These diagrams are based on the FAA flight-test results. An analytical procedure to approximate low hover height and rotor-speed characteristics at low hover height is presented in appendixes A and B, respectively, and a detailed numerical example illustrating the application of the semiempirical method is presented in appendix C.

SYMBOLS

A	rotor-disk area, ft^2 ($meters^2$)
A_b	total rotor-blade area, ft^2 ($meters^2$)
b	number of rotor blades
$c_{d,o}$	mean blade section drag coefficient
C_L	rotor lift coefficient
$C_{L,max}$	maximum rotor lift coefficient
C_T	thrust coefficient, out of ground effect
f	equivalent flat-plate drag area, ft^2 ($meters^2$)
g	gravitational acceleration constant, 32.2 ft/sec^2 (9.8 meters/$second^2$)
h	rotor height above ground, ft (meters)
h_{cr}	geometric height at V_{cr}, ft (meters)
h_{hi}	high hover height, ft (meters)
h_{lo}	low hover height, ft (meters)
h_r	rotor height above ground at power failure, ft (meters)
h_x	arbitrary geometric height, ft (meters)
H_D	density altitude, ft (meters)
HP_{req}	required horsepower
I_R	rotor rotating inertia, slug-ft^2 (kilograms-$meters^2$)
m	helicopter mass, slugs (kilograms)

n	thrust-weight ratio
P	power, ft-lb/sec (meter-newtons/second)
Q_d	main rotor torque before power failure, ft-lb (newton-meters)
R	rotor-blade radius, ft (meters)
t	time, seconds
Δt	time from power cut to touchdown, seconds
T	rotor thrust, lb (newtons)
v	induced velocity in ground effect, ft/sec (meters/second)
V	forward speed, knots
V_{cr}	speed above which a power-off landing can be made at any height, knots
V_{min}	forward speed for minimum power, knots
V_t	rotor tip speed, ft/sec (meters/second)
$V_{V,d}$	landing-gear design vertical impact speed, ft/sec (meters/second)
V_x	arbitrary airspeed associated with h_x
W	aircraft weight, lb (newtons)
X	nondimensionalizing ratio for height-velocity curve
μ	tip-speed ratio
ρ	ambient air density at any altitude, slug/ft^3 (kilogram/meters^3)
ρ_o	ambient air density at sea level, slug/ft^3 (kilogram/meters^3)
Ω	rotor speed, radians/second^2

Ω_d design rotor speed, radians/second

Ω_f final rotor speed at touchdown, radians/second

Λ ground effect parameter, $\frac{\text{Power in ground effect}}{\text{Power out of ground effect}}$

σ solidity, A_b/A

Subscripts:

avg average

ff free-fall height

o initial condition

SL conditions at sea level

∞ out of ground effect

1 upper portion of the nondimensionalized curve

2 lower portion of the nondimensionalized curve

5000 conditions at 5000 ft (1524 meters)

9000 conditions at 9000 ft (2743 meters)

The notations $\dot{}$ and $\ddot{}$ represent the first and second derivative, respectively.

TEST EQUIPMENT AND PROCEDURES

The three single-rotor helicopters chosen for this study represent a wide range in disk loading and rotor inertia and utilize two different types of landing gears. These physical characteristics were chosen to insure that the final test results would reflect a range of aircraft parameters and would not be limited to one specific helicopter configuration. In addition to determining the effects of variations in the configuration, some insight into various control techniques was expected to be obtained.

The helicopters used in this investigation are shown in figure 2. In all further discussion the test helicopters are referred to by the designations in figure 2. All tests were conducted in a manner similar to the tests in references 4 to 6, that is, the pilot flew over the test course and repeatedly simulated power failure at a specified airspeed and at progressively lower heights or at constant heights and progressively lower airspeeds. From the point of similated engine failure, the pilot maneuvered the helicopter to obtain the best combination of airspeed, rotor speed, and rate of descent to effect a landing. In his judgment, this combination represented the maximum utilization of available energy without damaging the aircraft. This flight procedure continued until a combination of height and airspeed was reached which, in the pilot's opinion, represented a maximum performance point. The tests were flown by skilled test pilots; therefore, the resulting height-velocity diagrams should not be considered to be representative for the average pilot.

In general, the high-speed low-height portion of the restricted flying region (fig. 1) was not investigated during the present experimental flight tests because density altitude and gross weight are probably the least important of the many factors affecting this region. Consequently, this area is not subjected to analytical treatment in this report.

Other important parameters reflected in the data obtained from the FAA tests are terrain, wind, and airspeed conditions. Although terrain has no aerodynamic effect on the height-velocity diagram, it is an important factor for the pilot to consider when making an autorotative landing. Because debris on the landing site may cause damage to the helicopter, a poor landing surface can affect the pilot's ability to make a high performance power-off landing. The referenced tests were made on terrain which included both unpaved landing surfaces with hidden rocks immediately below the surface soil and on narrow crowned paved strips of rough composition. The airspeed was recorded on a flight-path analyzer and represents a ground speed. All tests were conducted at wind velocities under 5 miles per hour (2.24 meters per second).

ASSUMPTIONS

The semiempirical procedure and the analysis of significant test results described in the succeeding paragraphs are governed by the following assumptions: (a) The range of design mean lift coefficients varies from approximately 0.31 to 0.60, (b) no rotors with gross design differences (such as tip jets) are considered, (c) there are no radical differences in the landing-gear configuration or pilot position which would alter the energy-absorption capabilities or pilot visibility from the three test aircraft, (d) tests are not conducted at density altitudes or gross weights where the maximum collective pitch needed for autorotation needed to be greater than the pitch permitted by the placard rotor

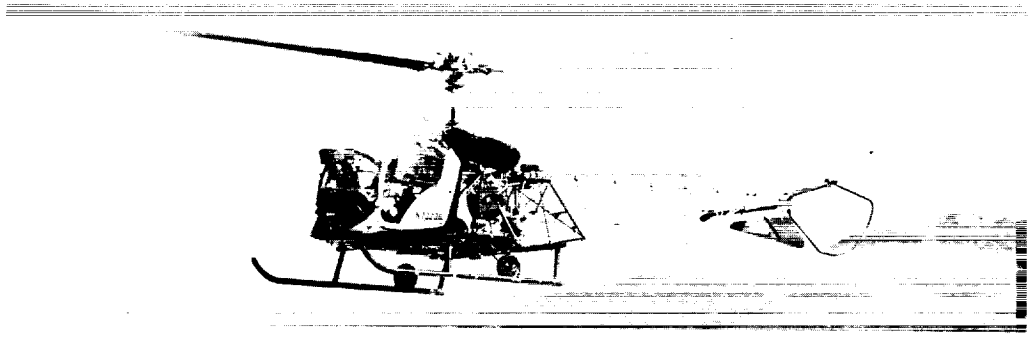

(a) Helicopter A. L-68-814

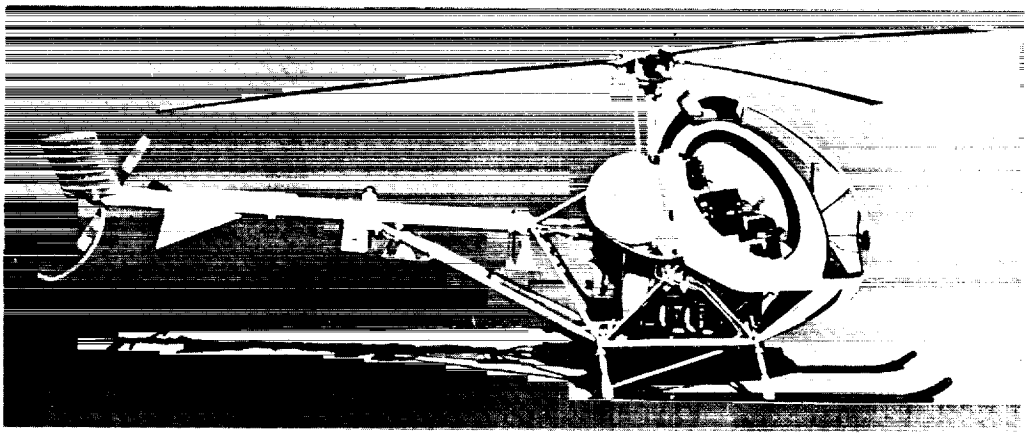

(b) Helicopter B. L-68-815

(c) Helicopter C. L-68-816

Figure 2.- Test aircraft.

speed limit, (e) the effects of adverse handling characteristics on the height-velocity diagrams is assumed to have been minimized because of the high proficiency level of the pilot with his individual helicopter, and (f) the results are applicable within a range of disk loadings from approximately $2\frac{1}{2}$ to 5 lb/ft^2 (120 to 239 N/m^2) and a range of density altitudes from approximately -1000 to 11 000 feet (-305 to 3353 m).

RESULTS AND DISCUSSION

Flight-Test Results

The primary results of the tests reported in references 4 to 6 are shown in the variation of the height-velocity diagrams with density altitude and gross weight for three different helicopters (fig. 2). A summary of this information is presented in figure 3. Figure 3(a) shows the variation of the height-velocity diagrams with aircraft gross weight, and figure 3(b) shows the effect of increases in density altitude on the height-velocity diagrams. These diagrams and similar diagrams form the experimental basis for this report.

Generalization of Height-Velocity Diagrams

The flight-test data of references 4 to 6 indicate that the three combinations of height and airspeed (h_{lo}, h_{hi}, V_{cr}, and h_{cr}) were linearly related with weight and density altitude and that the height-velocity diagrams of all the helicopters tested were of similar shape. By using suitable scaling factors, one generalized height-velocity curve could be obtained for all the test helicopters regardless of density altitude or gross weight. This information forms the basis for the following height-velocity diagram analysis.

Scaling of the height-velocity diagram is based on three combinations of height and airspeed. Once these three combinations are fixed, the entire height-velocity diagram may then be drawn. A generalized nondimensional height-velocity curve is shown in figure 4.

The two scaling parameters used in this analysis are functions of the heights h_{lo}, h_{hi}, h_{cr}, and the airspeed V_{cr}. They represent fractions of vertical distance up from h_{lo} to h_{cr} and down from h_{hi} to h_{cr}. The two parameters are defined as follows and are shown in figure 4.

$$X_1 = \frac{h_{hi} - h_{x_1}}{h_{hi} - h_{cr}}$$

$$X_2 = \frac{h_{x_2} - h_{lo}}{h_{cr} - h_{lo}}$$

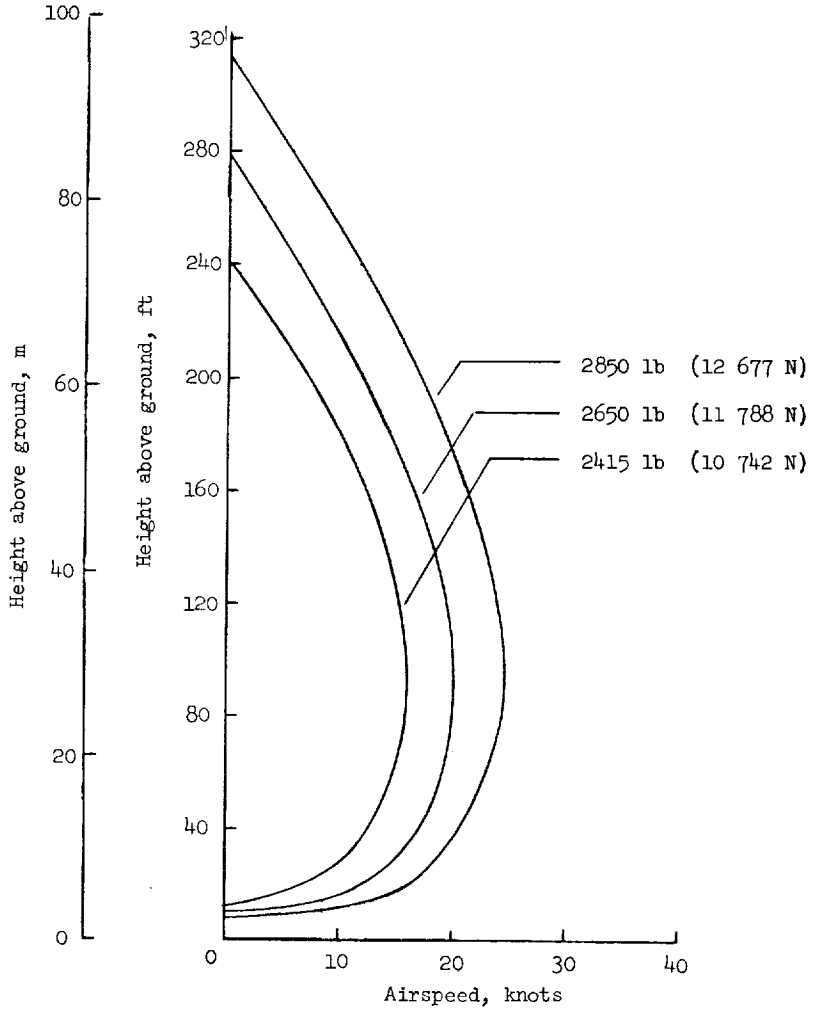

(a) Height-velocity diagram variation with gross weight.
Average density altitude sea level.

Figure 3.- Height-velocity diagrams obtained from reference 4 for helicopter A.

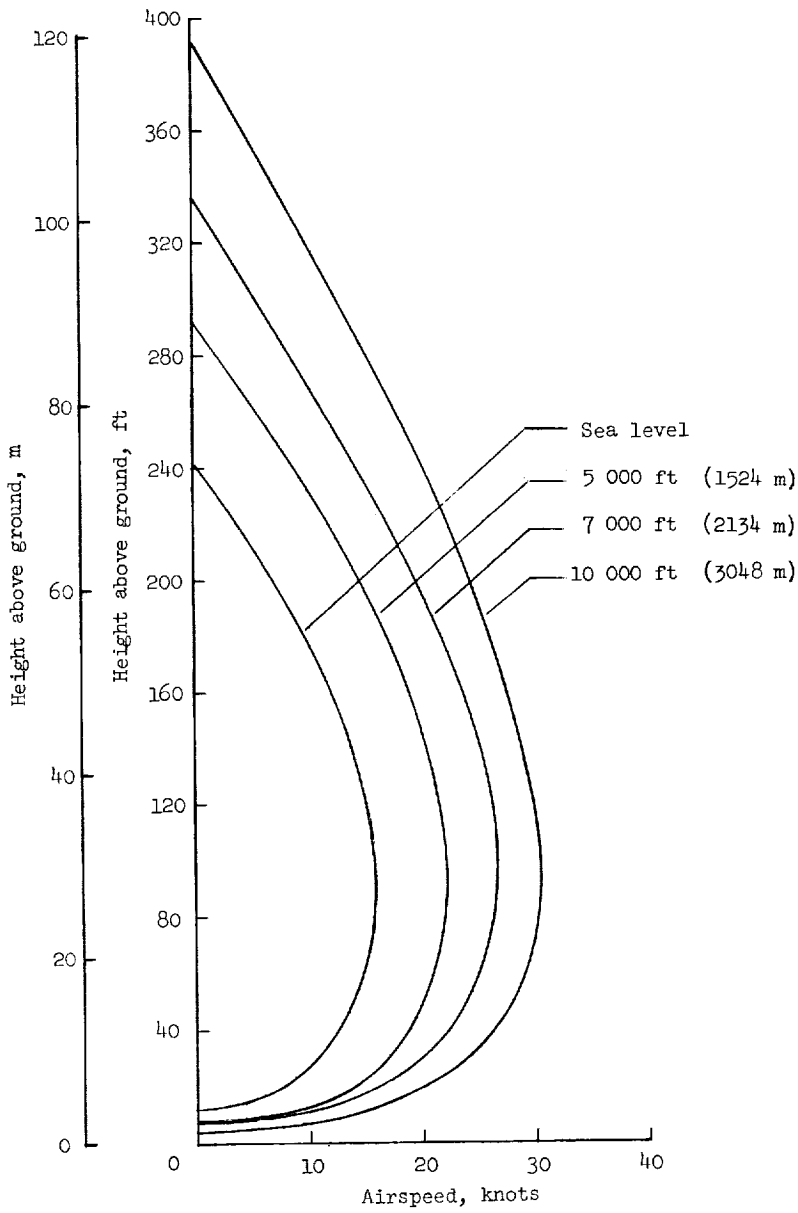

(b) Height-velocity diagram variation with density altitude. Gross weight 2415 lb (10 742 N).

Figure 3.- Concluded.

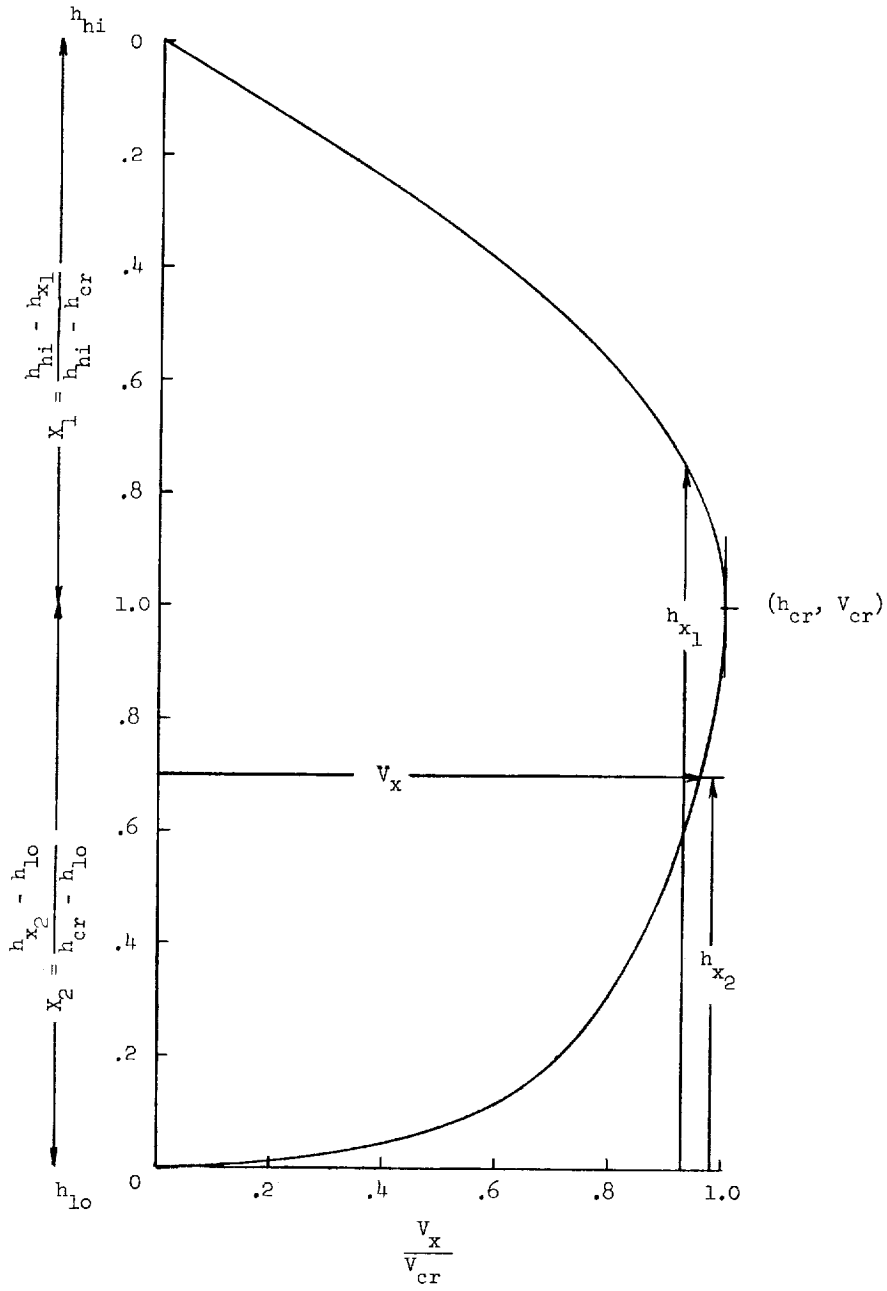

Figure 4.- Generalized nondimensional height-velocity curve.

The data shown in figure 3 and in references 4 to 6 are scaled and replotted in figure 5. Comparison of the three parts of figure 5 shows that a summary height-velocity curve can be obtained. This curve is independent of variations in gross weight and density altitude and is shown in figure 6. The good agreement shown in figure 6 for the three configurations, regardless of density altitude or gross weight, indicates that the scaling factors were well chosen.

Required Height-Airspeed Combinations

The three combinations of height and airspeed which must be determined before an actual height-velocity diagram is transformed into a height-velocity curve or vice versa by the method used herein are defined as follows:

(a) The low hover height h_{lo} is that height below which a safe autorotative landing can be made after a power failure at zero airspeed.

(b) The high hover height h_{hi} is that height above which a safe autorotative landing can be made after a power failure starting from zero airspeed.

(c) The midpoint V_{cr},h_{cr} is the maximum airspeed below which a safe autorotation cannot be made when initiated at h_{cr}.

These heights and airspeeds are indicated on the height-velocity diagram in figure 1.

Determination of Height-Airspeed Combinations

To draw a specific height-velocity diagram based on the generalized height-velocity curve, the values for the height and airspeed at the low hover height, high hover height, and midpoint must be determined.

Flight-test method.- Flight-test data obtained from height-velocity diagrams representing at least two gross weights at one density altitude must be used to determine the following necessary parameters and relationships:

(a) To determine the variation of the low hover height with gross weight and density altitude, the low hover height equation (see appendix A for derivation) must be evaluated. An accurate evaluation of this equation depends primarily on the rotor speed characteristics (variation of Ω_f/Ω_d and C_T/σ with Δt for the particular helicopter design).

(b) As indicated by FAA flight-test data, the variation of critical height with gross weight and density altitude at the midpoint of the height-velocity diagram remains at approximately 95 feet (29 meters). This approximation should be checked with flight-test results. The corresponding airspeed at the midpoint V_{cr} is determined by

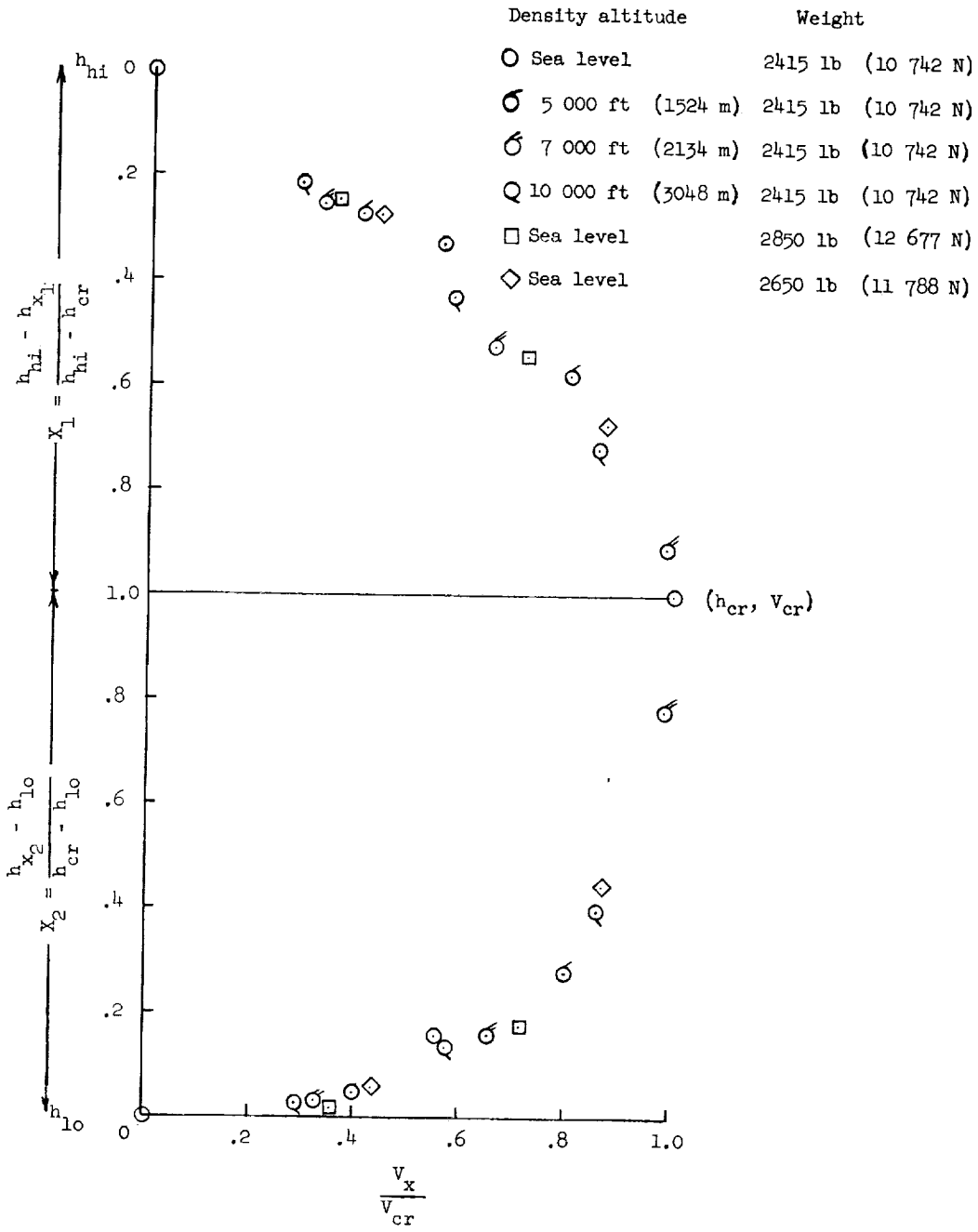

(a) Helicopter A.

Figure 5.- Nondimensional height-velocity curves for the test helicopters.

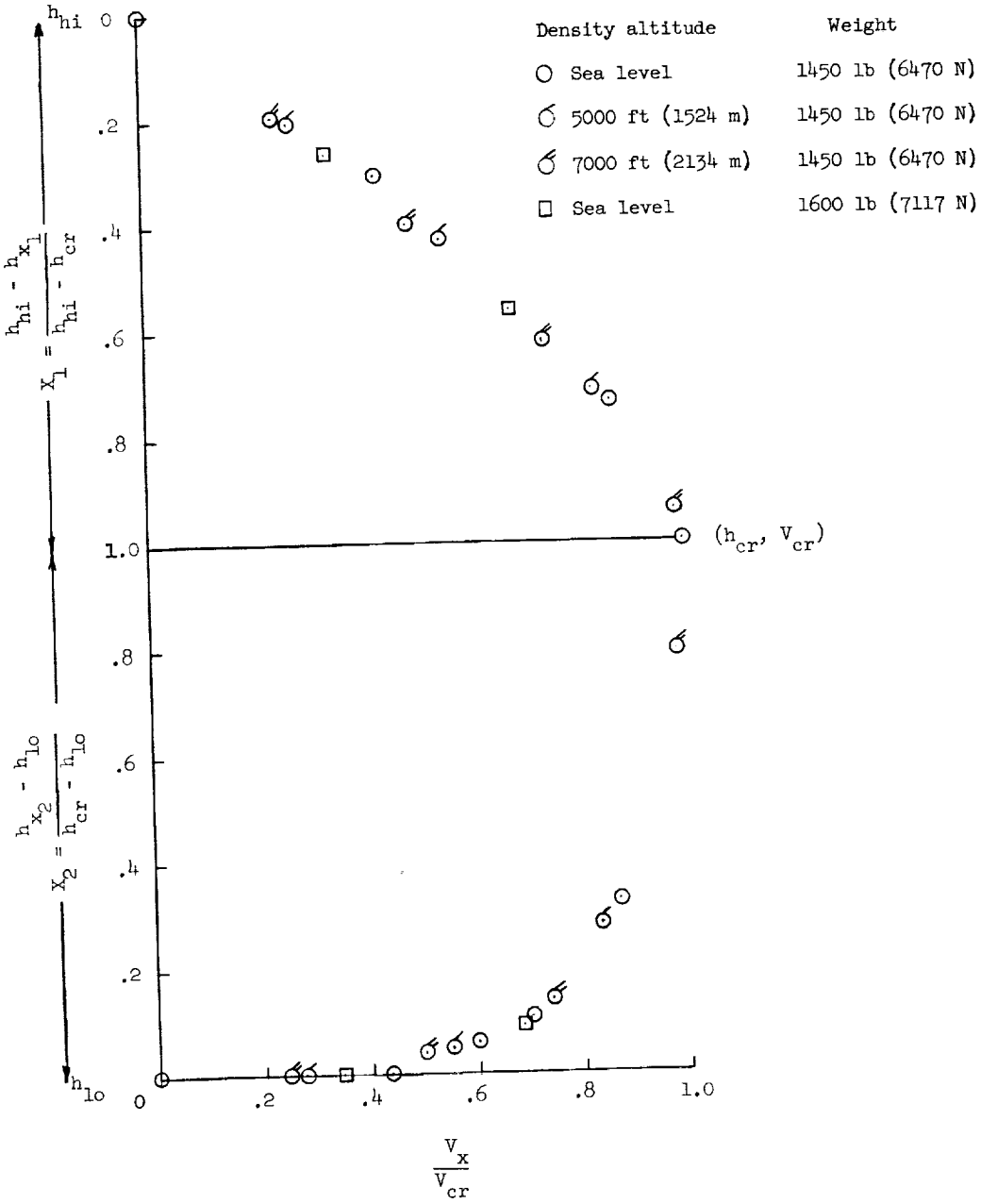

(b) Helicopter B.

Figure 5.- Continued.

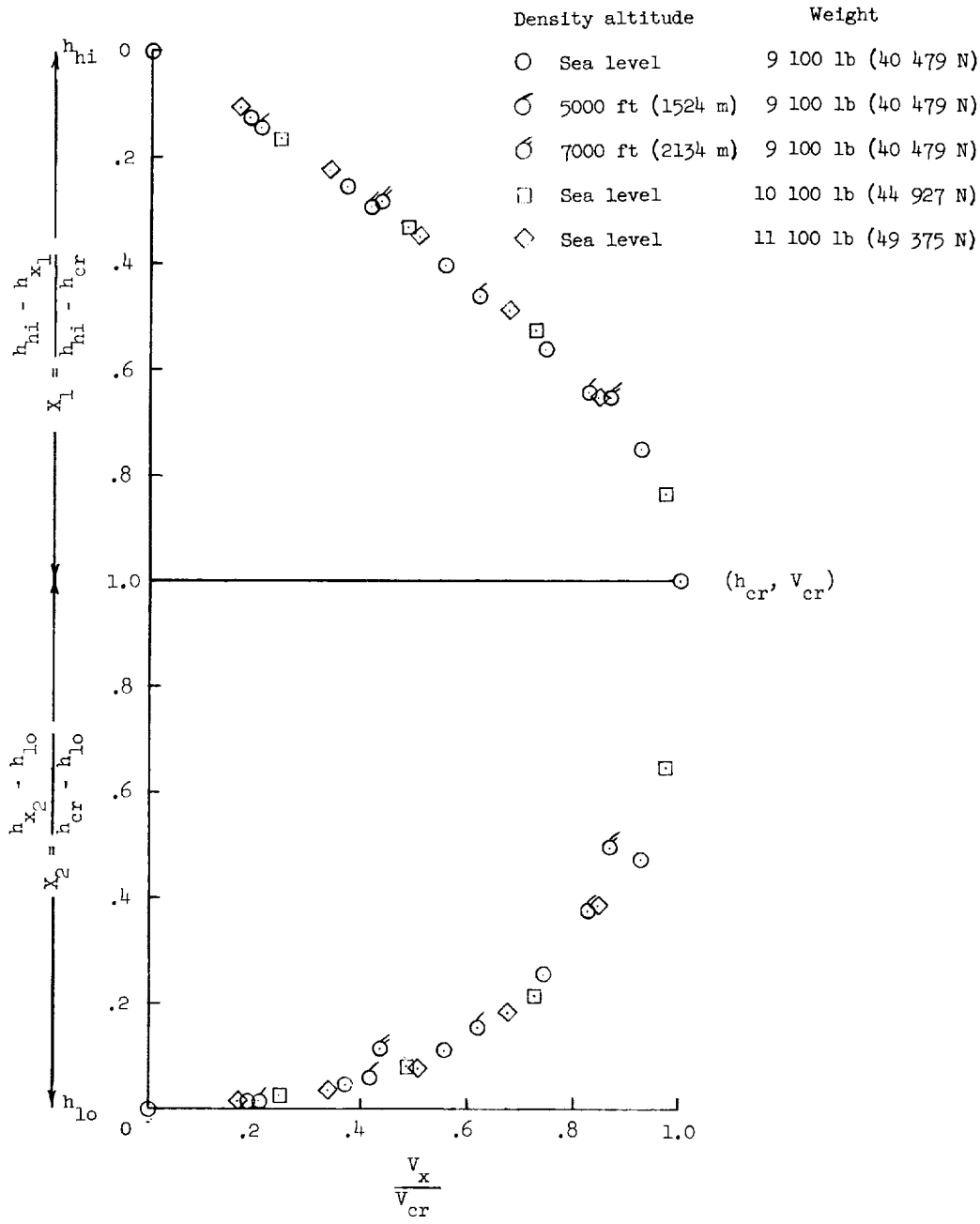

(c) Helicopter C.

Figure 5.- Concluded.

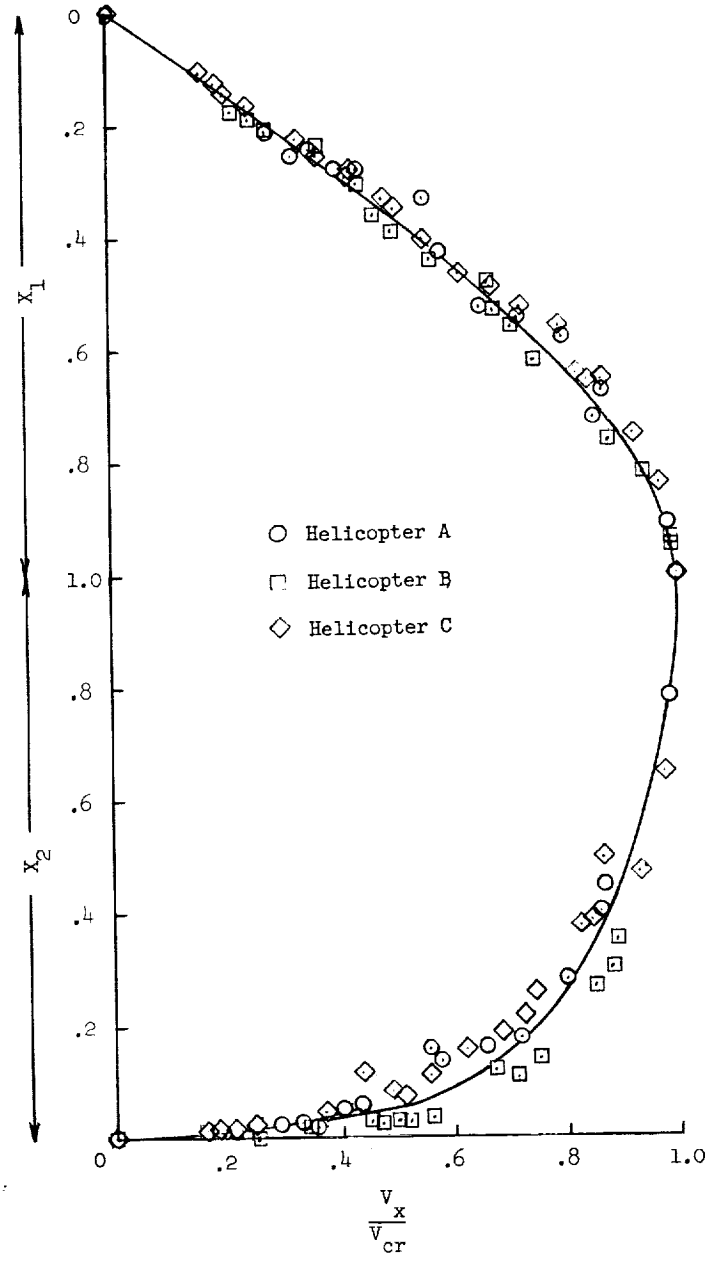

Figure 6.- Summary height-velocity curve for helicopters A, B, and C.

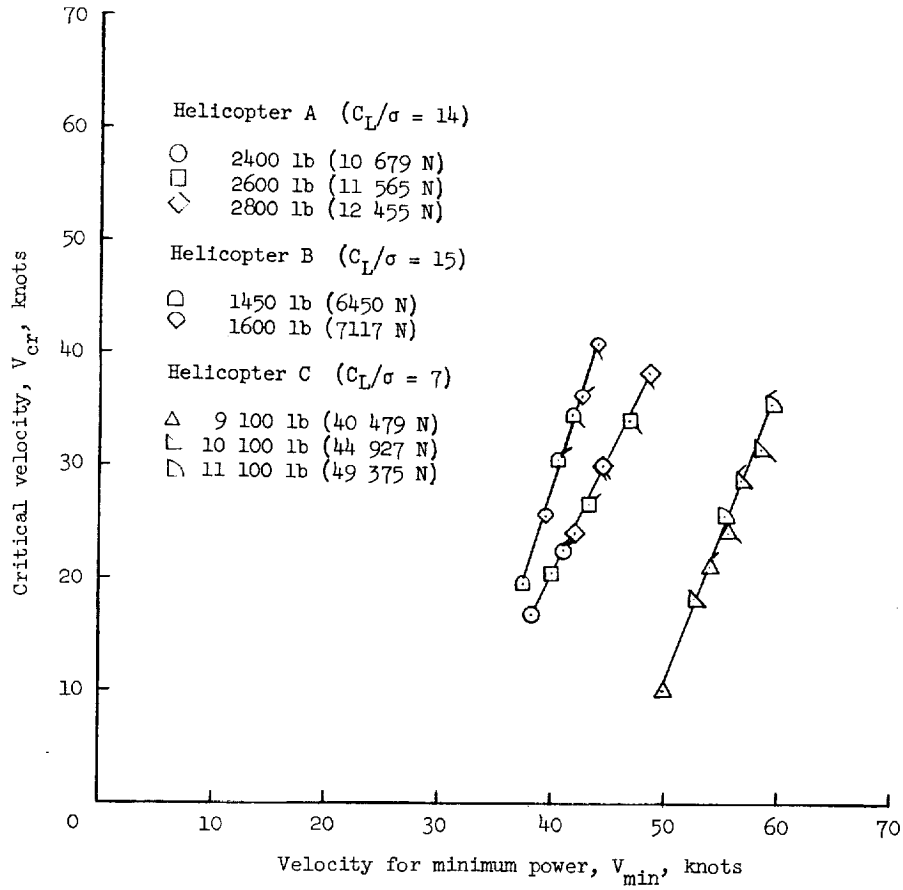

Figure 7.- Variation of V_{cr} with V_{min} for the three test helicopters. Plain symbols indicate tests at sea level; flagged symbols at 5000 ft (1524 meters); tailed symbols at 6900 ft (2103 meters), except helicopter A at 10 000 ft (3048 meters).

obtaining a curve of the variation of V_{cr} to V_{min} similar to that shown in figure 7. From this relationship, V_{cr} may be determined at any gross weight and density altitude.

(c) The flight-test data obtained from the two height-velocity diagrams should yield high hover heights that conform generally to the curve in figure 8 which shows the variation of h_{hi} with V_{cr}^2.

The flight-test height-velocity diagrams for a particular helicopter, when appropriately scaled, provide the basis for extrapolations to different gross weights and density altitudes. The resulting height-velocity diagrams then reflect the same degree of accuracy as the initial flight-test data.

Semiempirical procedure.- A first-order approximation of the various parameters needed to show the variation of the height-velocity diagram with gross weight and density

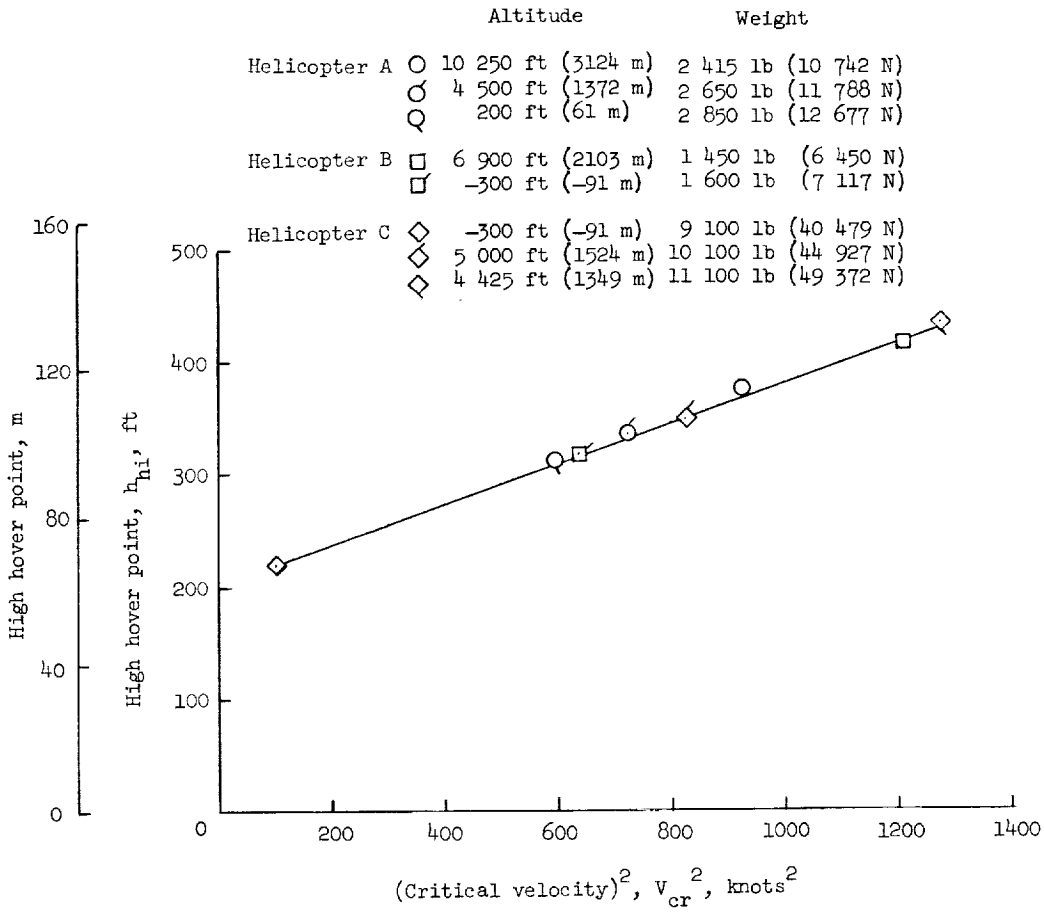

Figure 8.- Variation of h_{hi} with V_{cr}^2 taken from FAA flight-test data.

altitude may be made with the experimental FAA flight-test data and mathematical expressions derived in appendix B.

(a) The low hover height may be calculated by using the equations derived in appendix A; however, the variation of Ω_f/Ω_d with C_T/σ can be expressed as

$$\frac{\Omega_f}{\Omega_d} = 2.24\sqrt{C_T/\sigma}$$

and the variation of Ω_f/Ω_d with Δt may be expressed as

$$\Delta t = \left(1 - \frac{\Omega_f}{\Omega_d}\right)\frac{I_R\Omega_d^2}{550HP_{req,\infty}\Lambda}$$

This last expression is approximate because the collective pitch is assumed to be held constant. A mean value of the ground effect is shown in figure 9.

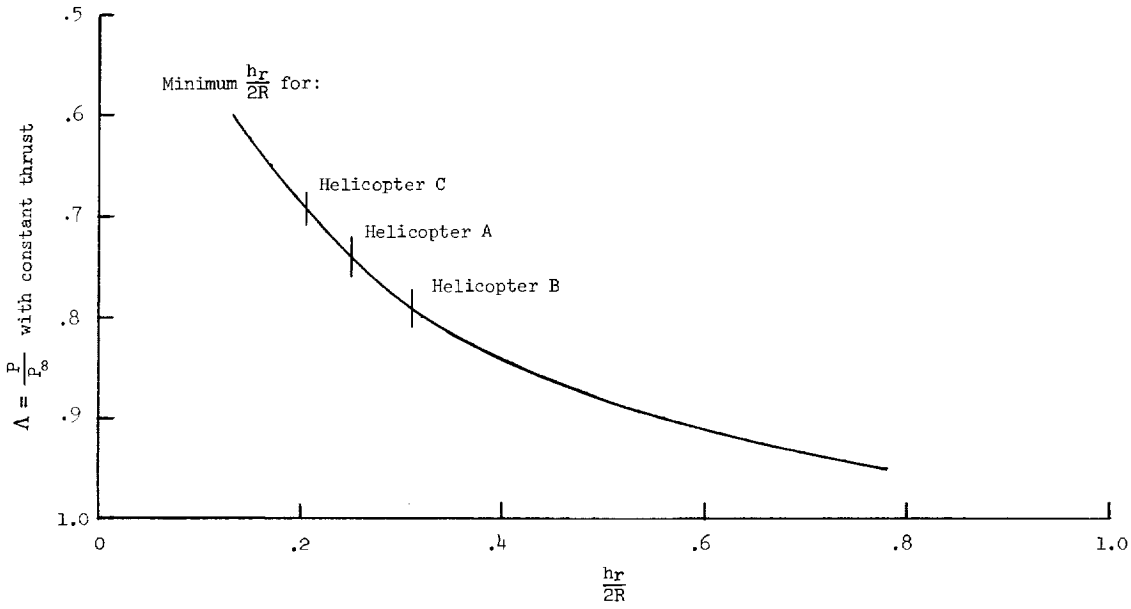

Figure 9.- Ground effect as determined from the experimental data of reference 10.

(b) The airspeed at the midpoint of the height-velocity diagram may be estimated from figure 10 which shows the variation of V_{cr} with V_{min} at various values of C_L/σ. Figure 10 is extrapolated from the flight-test data of references 4 to 6 and C_L/σ is the expression presented in reference 8 (p. 231) as

$$\frac{C_L}{\sigma} = \frac{2}{\mu^2}\frac{C_T}{\sigma}$$

where μ is the tip speed ratio at V_{min}. The critical height at the midpoint is taken as 95 feet (29 meters).

(c) Because of the excellent correlation of the FAA flight-test data, as shown in figure 8, figure 10 is assumed to be sufficiently accurate for conventional helicopters which fall within the range of variables covered by the FAA tests.

The method presented in this section is illustrated by a sample problem in appendix C.

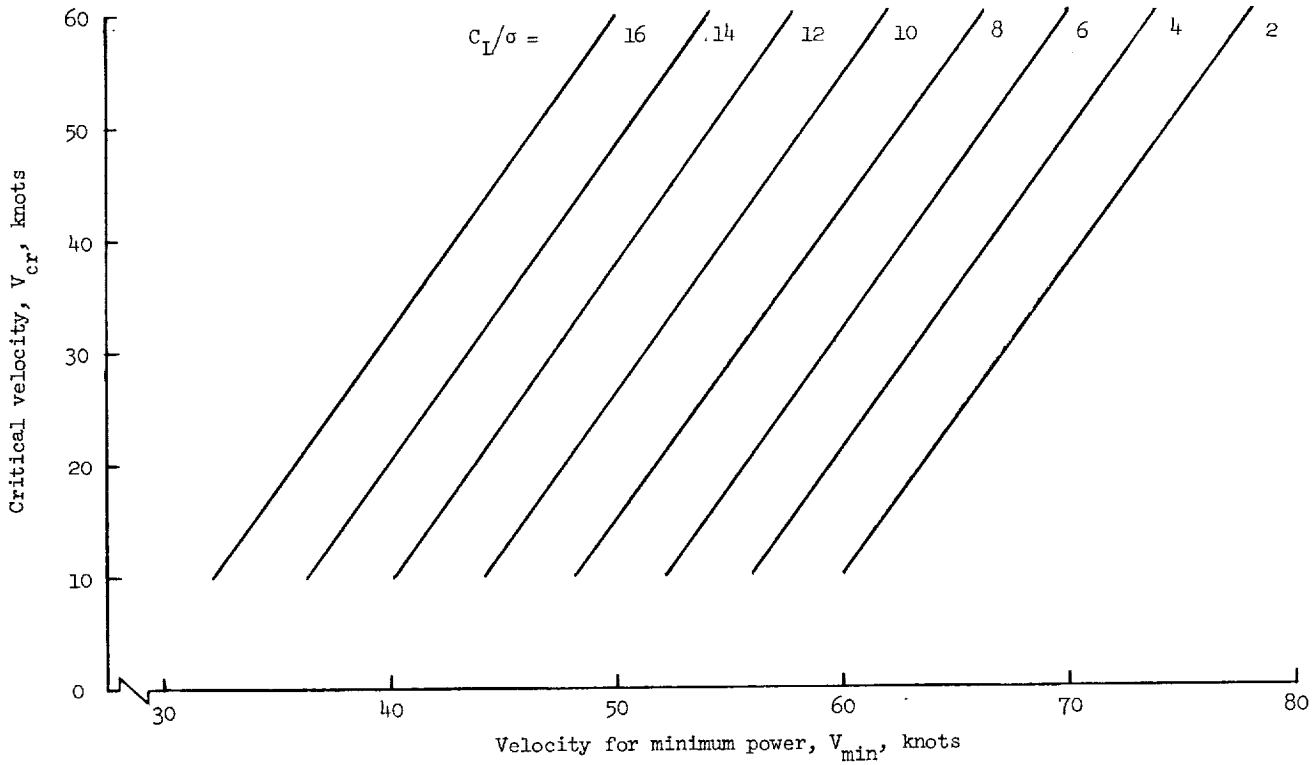

Figure 10. Variation of V_{cr} with V_{min} (modified for design use).

CONCLUDING REMARKS

The semiempirical method presented in the present report provides a means of using helicopter height-velocity flight-test data for a particular configuration taken, for example, at one density altitude and several weights to obtain height-velocity diagrams at other weights and density altitudes. The method also provides a means of determining approximate height-velocity diagrams (aside from those characteristics attributable to handling qualities, landing-gear arrangement, and pilot visibility) during the preliminary design of the helicopter. In the latter case, however, proper use of the procedure requires a background of pertinent design data from other helicopters and an element of judgment based on experience.

Because of the semiempirical nature of the method for determining variations in helicopter height-velocity diagrams described in this report, certain basic limitations are inherent in the procedure:

(a) Height-velocity diagrams resulting from the use of this procedure are based on flight-test data obtained from very experienced test pilots and should not be used in flight manuals as limitations for the average pilot.

(b) The height-velocity diagrams derived by using the method presented in this report minimize the influence of handling qualities, landing-gear arrangement, and field of vision.

Caution must be exercised when the method is extrapolated to higher altitudes (and higher mean lift coefficients) where tests were not conducted since stall, compressibility, and other aerodynamic effects will have an increased effect on the helicopter performance.

Langley Research Center,
National Aeronautics and Space Administration,
Langley Station, Hampton, Va., December 13, 1967,
721-06-00-06-23.

APPENDIX A

DERIVATION OF LOW HOVER HEIGHT

The low hover height equation is derived by summing vertical forces on the helicopter and equating these forces to the rate of change of vertical momentum. This technique may be used because an average value of maneuver load factor modifies the constant acceleration of gravity. This method, therefore, yields only a first-order solution to the problem and cannot be used to obtain time histories of the trajectories. However, the resulting equation does indicate the effect of density altitude and gross weight on the low hover height.

The aircraft is assumed to be initially hovering at some height above the ground. Figure 11 shows the forces acting on the helicopter. A summation of vertical forces yields the equation

$$m\ddot{h} = T - W$$

$$\ddot{h} = g(n - 1) \tag{A1}$$

Integrating equation (A1) gives the helicopter vertical velocity

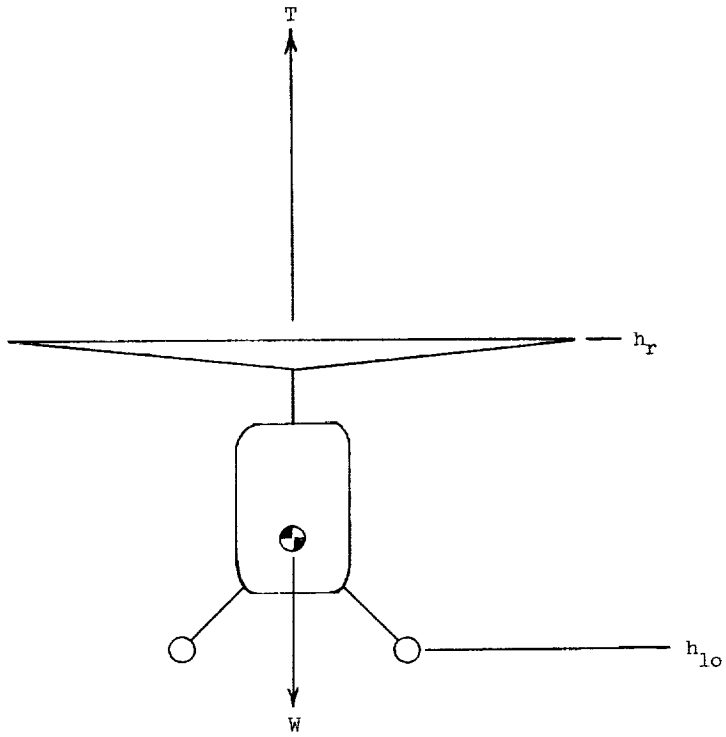

Figure 11.- Forces acting on the helicopter during the vertical power-off landing maneuver.

$$\dot{h} = \dot{h}_o + g(n - 1)t \tag{A2}$$

The helicopter vertical displacement is obtained by integrating equation (A2)

$$h_{lo} = h = \dot{h}_o \Delta t + g(n - 1)\frac{\Delta t^2}{2} \tag{A3}$$

The average maneuver load factor must now be evaluated. This evaluation may be made by one of two methods: (a) If a vertical impact speed is specified (landing-gear structural considerations), from equation (A2)

$$n_{avg} = \frac{V_{V,d}}{g\,\Delta t} + 1 \tag{A4}$$

(b) If some knowledge of the control inputs and their interrelation with rotor speed is available,

through a numerical integration of the thrust, the average load factor may be obtained as

$$n_{avg} = \frac{\int_0^{\Delta t} T\, dt}{W\, \Delta t} \tag{A5}$$

Proper collective pitch control inputs must be made in the thrust expression so that the average load factor results in impact velocities within the structural limitations of the landing gear.

By the use of the value of Δt (derived in appendix B)

$$\Delta t = \frac{I_R \Omega_d^2}{550 HP_{req,\infty} \Lambda}\left(1 - \frac{\Omega_f}{\Omega_d}\right) \tag{A6}$$

and the value of Ω_f/Ω_d as

$$\frac{\Omega_f}{\Omega_d} = 2.24\sqrt{C_T/\sigma} \tag{A7}$$

equation (A3) may be evaluated from equations (A4), (A6), and (A7)

$$h_{lo} = -\frac{I_R \Omega_d^2 V_{V,d}}{1100 HP_{req,\infty} \Lambda}\left(1 - 2.24\sqrt{C_T/\sigma}\right) \tag{A8}$$

The low hover height, as computed from equation (A8), does not indicate that a lower free-fall height limit exists. This free-fall height limit is determined by equating the kinetic and potential energies as follows:

$$\left.\begin{aligned} mgh_{ff} &= \frac{1}{2} m V_{V,d}^2 \\ h_{ff} &= \frac{V_{V,d}^2}{2g} \end{aligned}\right\} \tag{A9}$$

APPENDIX B

ROTOR-SPEED DECAY CHARACTERISTICS AT THE LOW HOVER HEIGHT

Analysis of the low hover height h_{lo} (defined in fig. 1) depends in part upon the ability of the designer to obtain a sufficiently accurate rotor-speed expression which is readily amenable to mathematical manipulation. Flight-test data are used to develop a method by which rotor decay characteristics may be estimated. The resulting expressions for Ω_f/Ω_d and Δt are then used in appendix A.

Figure 12 shows typical flight-test data from helicopter C which are useful in generalizing the analysis of the expression of the low hover height. Figure 12 is a time history of rotor speed and collective pitch during a vertical power-off descent within one rotor diameter of the ground. This figure shows that there is little apparent variation in

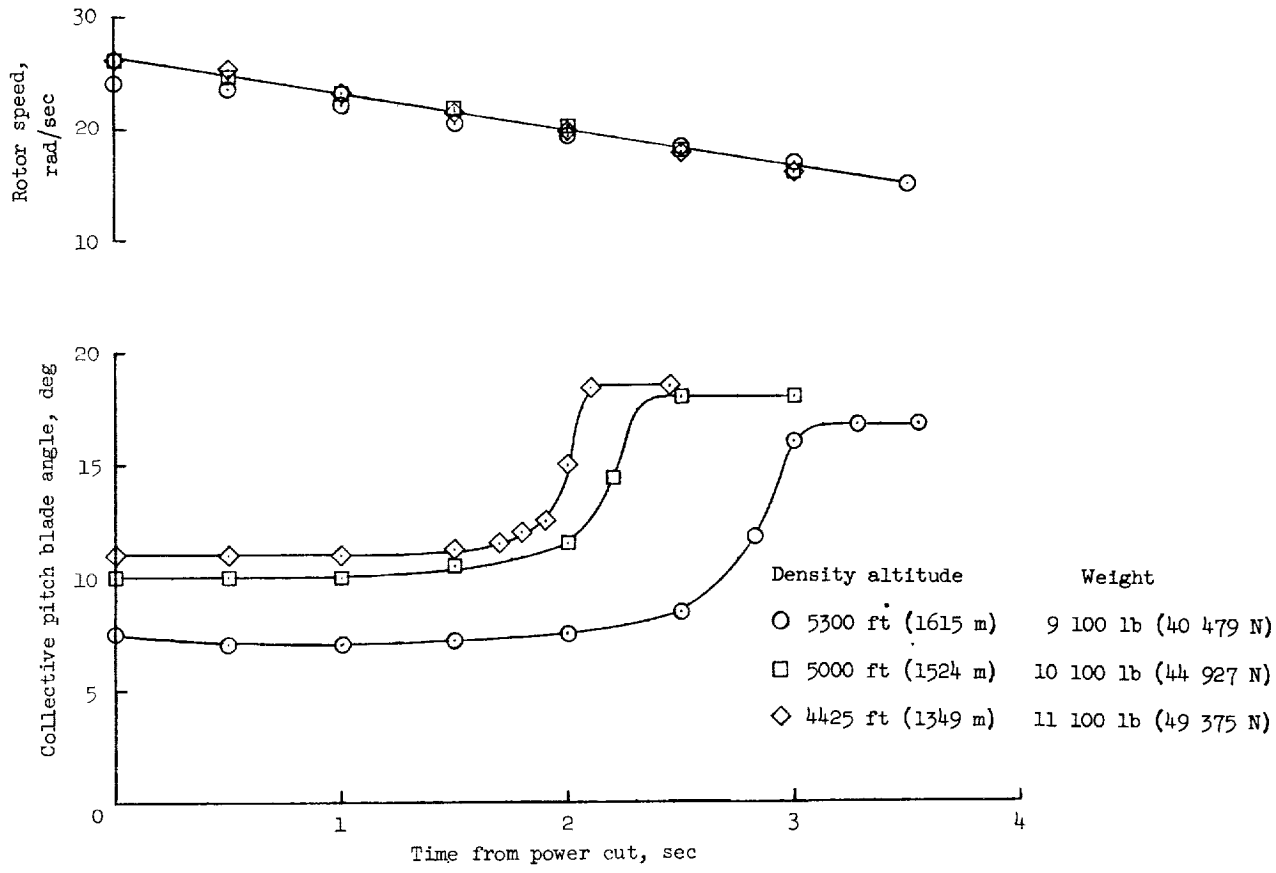

Figure 12.- Typical effect of collective control input on rotor-speed decay rate at the low hover point (helicopter C).

rotor-speed decay with the particular collective pitch inputs in ground effect. These inputs are typical of those found to be most expedient by the pilot. The data for this figure were taken from helicopter C; however, the indicated trends are representative of the other two test helicopters. These data are useful because they permit the use of one rotor-speed decay rate (dependent upon the configuration) when the collective control input retains the characteristics introduced in figure 12. The rotor-speed decay characteristics could be considerably modified if exceptionally high profile drag devices, such as tip jets, were installed on the rotor blades.

Two relationships used in the semiempirical analysis (appendix A) are the variations of Ω_f/Ω_d with C_T/σ and Δt. Figure 13 shows the variation of Ω_f/Ω_d with C_T/σ as derived from the FAA flight tests. In this semiempirical approach rotor geometry and control rigging are assumed to permit the rotor to attain a maximum lift coefficient of 1.2 at a $T/W = 1$. Therefore,

$$\frac{T}{W} = 1 = \frac{C_{L,max}\rho A\Omega_f^2 R^2}{\frac{6C_T}{\sigma}\rho A\Omega_d^2 R^2} \tag{B1a}$$

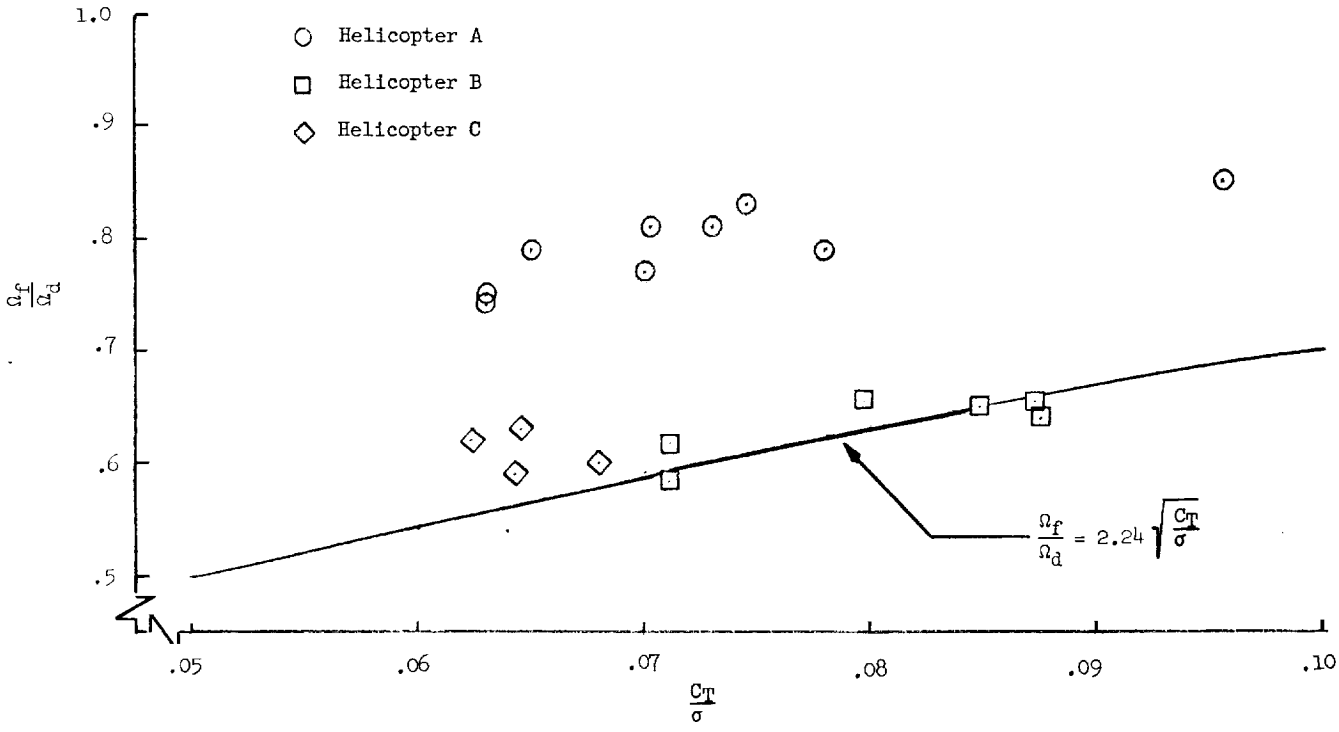

Figure 13.- Experimental variation of rotor speed ratio with c_T/σ; theoretical limit at $C_{L,max} = 1.2$.

$$\frac{\Omega_f}{\Omega_d} = \sqrt{\frac{6C_T/\sigma}{1.2}} = 2.24\sqrt{\frac{C_T}{\sigma}} \qquad \text{(B1b)}$$

This curve is indicated in figure 13. Although the results from helicopter A show that a $\sqrt{C_T/\sigma}$ relationship does exist, control rigging problems are believed to have prevented helicopter A from attaining maximum lift.

Once the value of Ω_f/Ω_d is determined from the trim conditions of the helicopter, the time interval from power failure to touchdown Δt may be estimated. The value of this time interval is obtained from a simplified statement of the rotor torque equation after a complete power failure and is modified to conform with the flight-test results shown in figure 14.

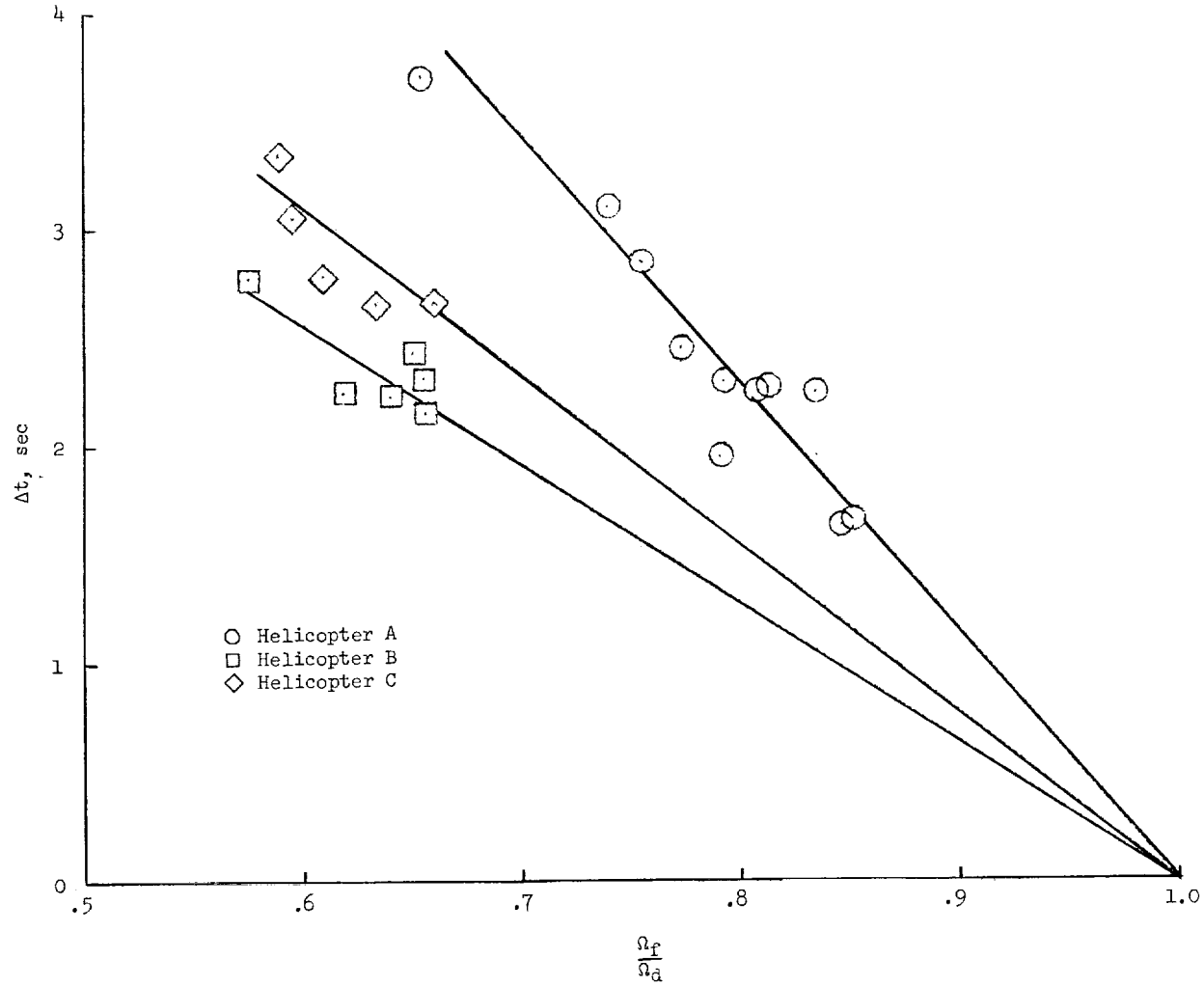

Figure 14.- Experimental variation of rotor speed ratio with time interval from power failure to impact at the low hover point.

APPENDIX B

$$I_R\dot{\Omega} = \Lambda Q_{d,\infty}\left(\frac{\Omega}{\Omega_d}\right)^2$$

$$d\Omega = \frac{\Lambda Q_{d,\infty}}{I_R}\left(\frac{\Omega}{\Omega_d}\right)^2 dt$$

$$\Delta t = \frac{I_R\Omega_d{}^2}{550HP_{req,\infty}\Lambda}\left(\frac{1}{\Omega_f/\Omega_d} - 1\right)$$

$$\frac{d\,\Delta t}{d\left(\frac{\Omega_f}{\Omega_d}\right)} = -\frac{I_R\Omega_d{}^2}{550HP_{req,\infty}\Lambda}$$

and by using the equation of a straight line

$$\Delta t = \left(1 - \frac{\Omega_f}{\Omega_d}\right)\frac{d\,\Delta t}{d\left(\frac{\Omega_f}{\Omega_d}\right)} \tag{B2}$$

This expression assumes constant collective pitch and is therefore only a valid approximation for the first 2 or 3 seconds of the power-off maneuver. Because of the simplified nature of equation (B2), it does not yield an accurate representation of the rotor-speed time history although it does approximate the time interval Δt adequately. Figure 14 shows the variation Δt with Ω_f/Ω_d for the three test helicopters.

APPENDIX C

NUMERICAL EXAMPLE

A numerical example is given here to illustrate the application of the semiempirical method outlined in the text for a helicopter at one gross weight and three density altitudes. The problem is (a) to determine h_{lo}, V_{cr}, h_{cr}, and h_{hi} for a given aircraft weight and density altitude, and (b) to use these values and the generalized nondimensional height-velocity curve to obtain the height-velocity diagram at the particular weight and altitude.

The following values are functions of the aircraft configuration:

$A = 960$ ft^2 (89.2 m^2)	$I_R = 760$ slug-ft^2 (1030.5 kg-m^2)	$W = 3700$ lb (13 656 N)
$f = 8$ ft^2 (0.74 m^2)	$R = 17.5$ ft (5.34 m)	$\sigma = 0.0591$
$b = 3$	$V_t = 650$ ft/sec (198.1 m/sec)	$\dot{\Omega} = -3.5$ radians/sec^2
$C_L/\sigma = 5.9$	$V_{V,d} = -8$ ft/sec (-2.44 m/sec)	$\Omega_d = 37.1$ radians/sec^2
$c_{d,o} = 0.013$	$h_r = 7.0$ ft (2.13 m)	

The following values are functions of density altitude.

H_D		C_T/σ	$HP_{req,\infty}$
ft	m		
Sea level	Sea level	0.0648	300
5000	1524	.0752	310
9000	2743	.0851	320

Equation (A8) is used with the appropriate values found in preceding portions to evaluate the low hover height as

$$h_{lo} = -\frac{I_R \Omega_d^2 V_{V,d}\left(1 - 2.24\sqrt{\frac{C_T}{\sigma}}\right)}{1100 HP_{req,\infty}\Lambda} = 7607.8\,\frac{\left(1 - 2.24\sqrt{\frac{C_T}{\sigma}}\right)}{HP_{req,\infty}\Lambda} \qquad \text{(C1)}$$

By using figure 9 and integrating the above equation, the following low hover heights are obtained:

$$(h_{lo})_{SL} = 12.1 \text{ ft} \quad (3.69 \text{ meters})$$

$$(h_{lo})_{5000} = 10.7 \text{ ft} \quad (3.26 \text{ meters})$$

$$(h_{lo})_{9000} = 9.4 \text{ ft} \quad (2.87 \text{ meters})$$

APPENDIX C

The forward airspeed for minimum power V_{min} may be obtained from performance calculations such as those given in reference 9 (ch. 6) for any desired weight or density altitude.

$$P_{required} = P_{induced} + P_{profile} + P_{parasite}$$

$$= \frac{1.13W^2}{2A\rho\left(V^2 + v^2\right)^{1/2}} + \frac{c_{d,o}A_b\rho V_t{}^3\left(1 + 3\mu^2\right)}{8} + \frac{\rho V_t{}^3 f}{2} \qquad \text{(C2)}$$

By taking the derivative of equation (C2) with respect to V, the equation for the forward speed for minimum power becomes

$$\frac{dP_{required}}{dV} = 0 = -\frac{1.13W^2}{2A\rho}\left[\frac{V_{min} + v\frac{dv}{dV}}{\left(V_{min}{}^2 + v^2\right)^{3/2}}\right] + 0.75c_{d,o}A_b\rho V_t V_{min} + 1.5\rho V_{min}{}^2 f \qquad \text{(C3)}$$

where dv/dV can be obtained from figure 77 of reference 9.

For the sample helicopter, equation (C3) becomes

$$\frac{-3.37 \times 10^6}{\rho/\rho_o}\frac{V_{min} + v\frac{dv}{dV}}{\left(V_{min}{}^2 + v^2\right)^{3/2}} + 0.86V_{min}\left(\frac{\rho}{\rho_o}\right) + 0.029V_{min}{}^2\left(\frac{\rho}{\rho_o}\right) = 0 \qquad \text{(C4)}$$

From this equation, the values of V_{min} are found by trial and error to be

$$(V_{min})_{SL} = 57.5 \text{ knots}$$

$$(V_{min})_{5000} = 62.3 \text{ knots}$$

$$(V_{min})_{9000} = 66.4 \text{ knots}$$

From figure 10 the following values of V_{cr} are obtained for $C_L/\sigma = 5.9$

$$(V_{cr})_{SL} = 24.0 \text{ knots}$$

$$(V_{cr})_{5000} = 37.5 \text{ knots}$$

$$(V_{cr})_{9000} = 49.0 \text{ knots}$$

The critical height is assumed to be constant at approximately 95 ft (28.7 meters) for all gross weights and density altitudes. This height is assumed to be the mean height for the scatter indicated by flight-test data.

By using the critical velocities presented previously and the linear curve of figure 8, three values of h_{hi} are obtained.

$$(h_{hi})_{SL} = 303 \text{ ft} \quad (92 \text{ meters})$$

$$(h_{hi})_{5000} = 454 \text{ ft} \quad (137 \text{ meters}) \quad \text{(extrapolated data)}$$

$$(h_{hi})_{9000} = 635 \text{ ft} \quad (194 \text{ meters}) \quad \text{(extrapolated data)}$$

The values of h_{lo}, h_{hi}, V_{cr}, and h_{cr} are now used to find the height-velocity diagram. This is done by substituting the appropriate values in the ratios which comprise the ordinate scale of figure 6. These ratios are rearranged in the following form:

$$h_{x_1} = X_1(h_{cr} - h_{hi}) + h_{hi}$$

$$h_{x_2} = X_2(h_{cr} - h_{lo}) + h_{lo}$$

At each value of V_x/V_{cr} the arbitrary height h_x is evaluated, and the height-velocity diagram is generated from the resulting points. (See fig. 15.) Since the example included three altitudes, figure 15 shows the effect on the height-velocity diagram of changing density altitude at one gross weight.

APPENDIX C

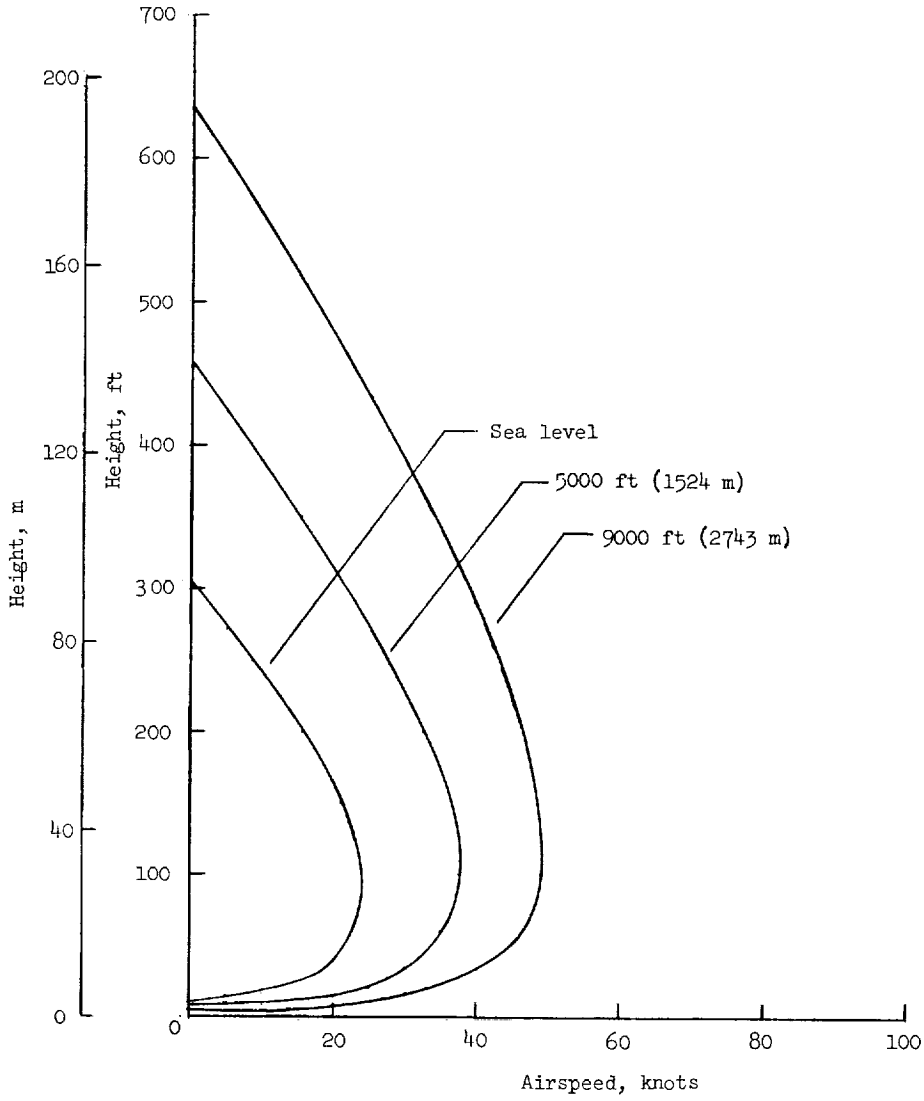

Figure 15.- Effect of density altitude on the height-velocity diagram for an aircraft weighing 3700 lb (16 458 N).

REFERENCES

1. Rich, M. J.: An Energy Absorption Safety Alighting Gear for Helicopter and VTOL Aircraft. Paper No. 62-16, Inst. Aerospace Sci., Jan. 1962.

2. Jepson, W. D.: Some Considerations of the Landing and Take-Off Characteristics of Twin Engine Helicopters. Part I – Height-Velocity Diagrams and Part Power Descents. J. Am. Helicopter Soc., vol. 7, no. 4, Oct. 1962, pp. 33-37. Part II – Heliport Size Requirements. J. Am. Helicopter Soc., vol. 8, no. 2, Apr. 1963, pp. 35-50.

3. Katzenberger, E. F.; and Rich, M. J.: An Investigation of Helicopter Descent and Landing Characteristics Following Power Failure. J. Aeron. Sci., vol. 23, no. 4, Apr. 1956, pp. 345-356.

4. Hanley, William J.; and DeVore, Gilbert: An Evaluation of the Effects of Altitude on the Height-Velocity Diagram of a Single Engine Helicopter. Tech. Rept. ADS-1, FAA, Feb. 1964.

5. Hanley, William J.; and De Vore, Gilbert: An Evaluation of the Height Velocity Diagram of a Lightweight, Low Rotor Inertia, Single Engine Helicopter. Tech. Rept. ADS-46, FAA, July 1965.

6. Hanley, William J.; DeVore, Gilbert; and Martin, Shirrel: An Evaluation of the Height Velocity Diagram of a Heavyweight High Rotor Inertia, Single Engine Helicopter. Tech. Rept. ADS-84, FAA, Nov. 1966.

7. Hanley, William J.; and DeVore, Gilbert: An Analysis of the Helicopter Height-Velocity Diagram Including a Practical Method for Its Determination. Tech. Rept. ADS 67-23, FAA, Oct. 1967.

8. Gessow, Alfred; and Meyers, Garry C., Jr.: Aerodynamics of the Heliocpter. The MacMillan Co., c.1952.

9. Young, Raymond A.: Helicopter Engineering. Ronald Press Co., 1949.

10. Stepniewski, W. Z.: Introduction to Helicopter Aerodynamics. Rotorcraft Publishing Committee.

NASA-Langley, 1968 — 2 L-5817